Stem cell factor receptor induces progenitor and natural killer cell-mediated cardiac survival and repair after myocardial infarction

Bilal B. Ayach*†, Makoto Yoshimitsu‡, Fayez Dawood*, Mei Sun*, Sara Arab*, Manyin Chen*, Koji Higuchi‡, Christopher Siatskas‡, Paul Lee*, Hilda Lim*†, Jane Zhang*, Eva Cukerman*, William L. Stanford†§, Jeffrey A. Medin†‡, and Peter P. Liu*†¶

*Toronto General Hospital Research Institute and ‡Ontario Cancer Institute, University Health Network, Toronto, ON, Canada M5G 2C4; and §Institute of Biomaterials and Biomedical Engineering and †The Heart and Stroke/Richard Lewar Centre of Excellence, University of Toronto, Toronto, ON, Canada M5G 2C4

Communicated by David H. MacLennan, University of Toronto, Toronto, ON, Canada, December 21, 2005 (received for review August 22, 2005)

Inappropriate cardiac remodeling and repair after myocardial infarction (MI) predisposes to heart failure. Studies have reported on the potential for lineage negative, steel factor positive (*c-kit*$^+$) bone marrow-derived hematopoetic stem/progenitor cells (HSPCs) to repair damaged myocardium through neovascularization and myogenesis. However, the precise contribution of the *c-kit* signaling pathway to the cardiac repair process has yet to be determined. In this study, we sought to directly elucidate the mechanistic contributions of *c-kit*$^+$ bone marrow-derived hematopoetic stem/progenitor cells in the maintenance and repair of damaged myocardium after MI. Using *c-kit*-deficient mice, we demonstrate the importance of *c-kit* signaling in preventing ventricular dilation and hypertrophy, and the maintenance of cardiac function after MI in *c-kit*-deficient mice. Furthermore, we show phenotypic rescue of cardiac repair after MI of *c-kit*-deficient mice by bone marrow transplantation of wild-type HSPCs. The transplanted group also had reduced apoptosis and collagen deposition, along with an increase in neovascularization. To better understand the mechanisms underlying this phenotypic rescue, we investigated the gene expression pattern within the infarcted region by using microarray analysis. This analysis suggested activation of inflammatory pathways, specifically natural killer (NK) cell-mediated mobilization after MI in rescued hearts. This finding was confirmed by immunohistology and by using an NK blocker. Thus, our investigation revealed a previously uncharacterized role for *c-kit* signaling after infarction by mediating bone marrow-derived NK and angiogenic cell mobilization, which contributes to improved remodeling and cardiac function after MI.

hematopoetic stem progenitor cells | steel factor receptor | angiogenesis

Cardiovascular diseases are the leading cause of morbidity and mortality in the Western world. Prolonged periods of myocardial ischemia lead to extensive myocyte injury and extracellular matrix remodeling that, in turn, leads to ventricular dysfunction and heart failure (1). Myocardial infarction (MI) is associated with an intense inflammatory response and activation of the host innate immune program for inflammatory cell mobilization and cardiac repair and remodeling (2, 3). Recent data suggests that various types of lineage negative, c-kit positive (*lin*$^-$*c-kit*$^+$) bone marrow (BM)-derived cells, including hematopoetic stem/progenitor cells and mesenchymal stem cells, can repair damaged myocardium after MI and improve cardiac remodeling (4). In this context, it has been shown either by direct cell injection (5) or by inducing cell mobilization (6–8) that BM cells home to the site of injury, contribute to the local wound repair, and may eventually differentiate into new vessels and myocytes (5–8). Other studies have failed to confirm the latter observation (9, 10) but instead suggest a paracrine role of BM-derived cells to mediate repair (11, 12). Although the ideal cell population to affect cardiac repair and the innate mechanisms mediating functional improvement after MI is still to be determined, we sought to clarify the role of c-kit signaling in the mobilization and homing of cells remote from the heart for repair.

The steel factor receptor (*c-kit*) is a member of the tyrosine kinase family of receptors and is activated by stem cell factor/kit ligand. Ligand binding leads to receptor dimerization and activation of multiple downstream signaling pathways involved in target mobilization, antiapoptosis, and cell proliferation (13–15). In addition, recent findings report a possible role for c-kit and fetal liver kinase (Flt3) signaling in the mobilization of innate immune cells such as natural killer (NK) cells in the setting of neoplastic growth (16).

NK and dendritic cells are the innate immune system's early defense against foreign cells and autologous cells undergoing various forms of stress (17). NK cell activation and deactivation are regulated by various membrane-bound receptors controlling cell lysis and cytokine or chemokine release (18). *c-kit* has been reported to play a major role in NK cell production and mobilization. In the absence of *c-kit*, there is a deficiency in production and maturation of BM-derived NK cells, whereas reduced *c-kit* activity leads to a reduction of circulating NK cells (18).

Using c-kit-deficient and littermate-matched wild-type (WT) mice, we examined the role of the c-kit receptor in cardiac remodeling and repair after MI. We observed a worsening in cardiac dilation and function in c-kit-deficient mice compared with WT controls mice. We also rescued the c-kit cardiac repair deficiency with WT BM transplantation and observed increased mobilization of angiogenic and NK cells after MI.

Results

Deviancy of c-kit Signaling Resulted in Diminished Function and Remodeling After MI. At 35 days after MI, there was worse heart function and greater cardiac dilatation in null *c-kit* mutation *W/W-viable* (*W/W*^{v}) mice compared with WT (Fig. 1). Left ventricle (LV) end-systolic pressure (LVESP) was significantly decreased (Fig. 1*A*) compared with WT controls (Fig. 1*A*). LV end-systolic volume (LVESV) increased significantly in *W/W*^{v} mice compared with WT controls (Fig. 1*B*). Stroke volume, positive dp/dt, and negative dp/dt were also significantly different (Fig. 1 *D–F*). Heart-to-body weight ratio (Fig. 1*C*), septal wall thickness, and percentage of LV infarcted, and collagen content (Fig. 1 *G–I*; see also Table 2, which is published as supporting information on the PNAS web site) were significantly increased in *W/W*^{v} mice compared with WT, whereas LV thickness significantly decreased

Conflict of interest statement: No conflicts declared.

Abbreviations: BM, bone marrow; BMT, BM transplanted; LV, left ventricle; MI, myocardial infarction; NK, natural killer.

¶To whom correspondence should be addressed. E-mail: peter.liu@utoronto.ca.

www.pnas.org/cgi/doi/10.1073/pnas.0510997103

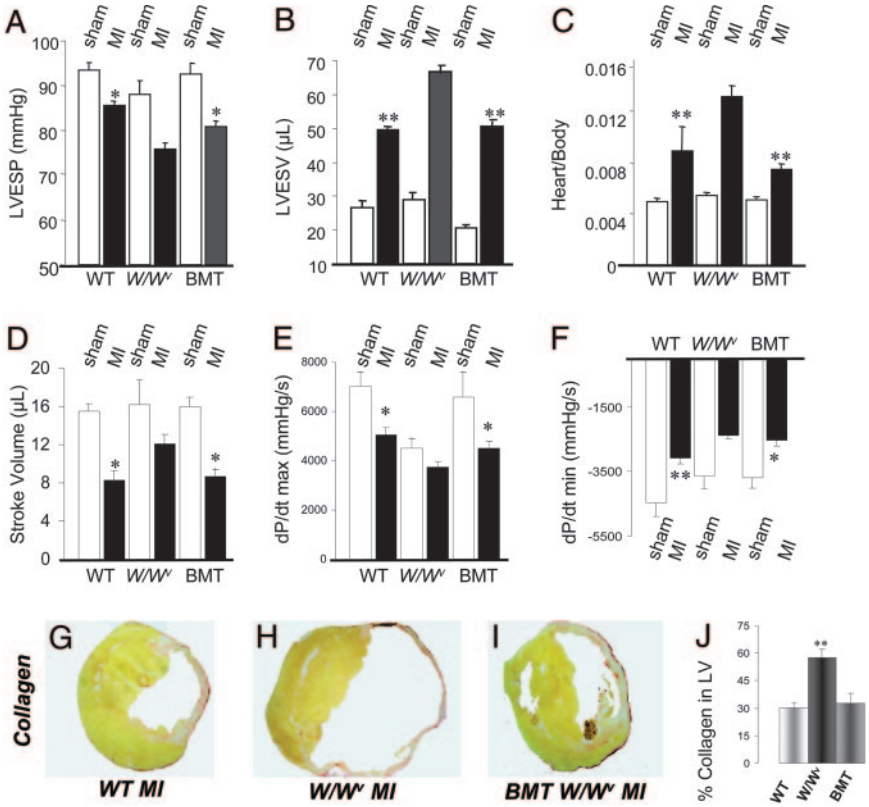

Fig. 1. Hemodynamic and morphometric analysis. (*A–F*) WT BMT W/W^v ($n = 11$) mice have significant improvement in LV end-systolic volume (LVESV), LV end-systolic pressure (LVESP), heart/body ratio, dP/dt max, and dP/dt min when compared with untreated W/W^v ($n = 9$). There also was a significant difference in stroke volume. (*G–J*) Collagen staining demonstrates BMT W/W^v parameters are rescued by WT BMT to levels comparable in WT mice ($n = 9$). There was no difference between shams ($n = 7$ each). Values are mean ± SEM. *, $P < 0.05$; **, $P < 0.001$.

in W/W^v mice (Table 2). There was no difference among sham groups.

BM Transplantation with WT Cells Rescues Defective Cardiac Repair in c-kit Mutants. WT BM transplanted (BMT) c-kit mutant mice rescued adverse cardiac remodeling and impaired cardiac function. Three months after irradiation and BMT with WT BM marked by EGFP provirus, 58 of 60 W/W^v transplanted mice survived and appeared well. Of these mice, 57 expressed demonstrable levels (>1%) of EGFP (ranging from 1.7% to 88.0% with a mean of 43.5 ± 2.8%) in peripheral blood after 3 months. Thirty-five days after MI, cardiac function was analyzed in a similar fashion as described above. All of these parameters were significantly improved in BMT W/W^v versus untreated W/W^v (Fig. 1 and Table 2), to levels comparable with those found in WT (Fig. 1 *A–I*). Transplantation of WT BM into W/W^v before MI prevented cardiac dilation and rescued worsening cardiac symptoms. There were no significant differences between sham-treated groups: W/W^v, WT, and BMT W/W^v (Fig. 1). There was no significant difference in flow analyses for CD4, CD8, CD19, Gr1, and CD11b, excluding either a significant rejection process or an exuberant T cell or B cell response.

Expression Analysis Highlights Critical c-kit Pathways in MI Recovery. Gene expression profiling depicted tight clustering between individual samples (W/W^v-untreated and the BMT W/W^v-treated group) (Fig. 2*A*). A total of 319 genes demonstrated differential expression at day 3 and 7 in BMT W/W^v vs. W/W^v and WT groups (258 up-regulated vs. 61 down-regulated). These genes were deemed as hypersensitive genes for this experiment, and a major functional cluster was identified as genes that regulate NK cell maturation and mobilization. Table 1 shows the functional clustering of genes based on the following: mobilization, apoptotic, angiogenic, and NK-related genes and markers. A full list of hypersensitive genes observed in this study are available upon request. Fig. 2*B* depicts differentially expressed (hypersensitive) NK-related genes and markers at day 3 and 7 BMT W/W^v vs. W/W^v and WT.

Immunohistochemistry Demonstrates c-kit Role in Cardiac Rescue. At 3 days after MI, greater numbers of inflammatory cells were observed in the peri-infarct region of WT and BMT W/W^v mice when compared to W/W^v mice alone. At day 35, inflammatory infiltration subsided, and necrotic tissue was replaced with fibrotic tissue. LV collagen content was greatest in W/W^v mice vs. BMT W/W^v and WT mice (57.5 ± 4.5% vs. 32.8 ± 5.2 and 30.3 ± 2.9%, respectively) (Fig. 1 *G–J* and Table 2). At day 3 and 7, TUNEL staining assay demonstrated a significantly greater level ($P < 0.001$) of nuclear damage and possible apoptosis in W/W^v hearts compared to WT and BMT W/W^v hearts. At day 3 after MI, 0.19 ± 0.02% vs. 0.064 ± 0.01% nucleated cells, and at day 7, 0.094 ± 0.01% vs. 0.038 ± 0.01%, indicating a significant ($P < 0.001$) increased cell death in the W/W^v group compared with BMT W/W^v mice (Fig. 7, which is published as supporting information on the PNAS web site). There were no observed differences in the rate of nuclear damage or apoptosis at day 35 after MI (data not shown). To analyze neoangiogenesis, $Ki67^+$ cells colocalized with CD31 demonstrated increased endothelial cell differentiation at the border zone of infarcted hearts at day 3 and 7 (Fig. 3 *A–G*). At day 35, the number of $Ki67^+$ cells decreased and there were no differences between the groups. However, there was a significant increase ($P <$ 0.001) in the number of vessels in the WT and BMT W/W^v

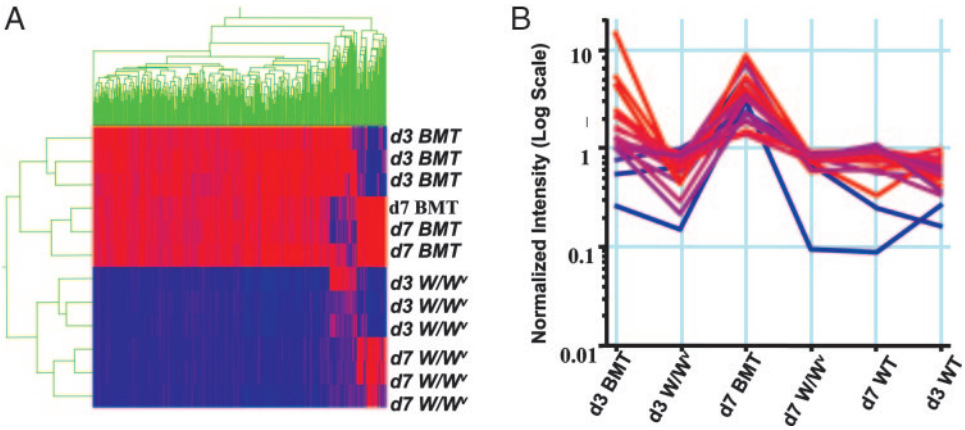

Fig. 2. Hierarchical clustering of differentially expressed genes in WT BMT W/W^v versus W/W^v ($n = 3$ each group). (*A*) Data filtering and two-way hierarchical cluster analysis identifies 319 genes that were differentially expressed in BMT W/W^v and not in W/W^v (hypersensitive genes). Gene expression levels are depicted as color variation (red, high expression; blue, low expression). (*B*) NK-related hypersensitive genes were significantly greater at 3 and 7 days after MI compared with all other groups (red, up-regulated at day 3 and 7; blue, only up-regulated at day 7).

compared with W/W^v untreated mice at day 35 after MI (Fig. 3*H*), suggesting increased angiogenesis in WT and rescued W/W^v mice.

Early Mobilization of BM Cells Contributing to Neovascularization. Monoclonal EGFP antibody staining was used to identify $EGFP^+$ cell presence in the normal zone, border zone, and infarcted regions of the heart. $EGFP^+$ expression was highest at day 3 and 7 after MI (30.7 ± 3.5 cells and 91.7 ± 8.6 cells, respectively). At these early time points, the $EGFP^+$ cells were small in diameter and did not have mature endothelial or myocyte morphology. However, at day 35 after MI, we found $EGFP^+$ BM-derived cells had contributed significantly to neovascularization (Fig. 4 *A–C*). We found no evidence of myogenesis by $EGFP^+$ cells.

NK Cell Mobilization and Engraftment in Rescued Mice. To determine the dominant mechanisms of rescue involved in the WT BM transplanted (BMT) mice, we used gene expression array analysis as a tool for pathway exploration. We observed hypersensitive gene clusters primarily expressed by NK cells that included the following: Klra, Klra8, Nkg7, CD94, and chemokine ligands cxcl9, cxcl10, and cxcl11 (19). Antibody staining for NK cell inhibitory receptor CD94 demonstrated significantly greater ($P < 0.001$) NK cell mobilization and engraftment in BMT W/W^v and WT groups versus W/W^v group (Fig. 4 *D–F*). The highest level of NK cell infiltration was observed at day 7 after MI in BMT W/W^v (Fig. 4*F*), and NK cells were absent at day 35. This observation demonstrates greater NK cell activity in the BMT W/W^v mice when compared with W/W^v and WT mice, and this data correlates with gene expression findings.

Higher FLT3L Expression After MI Reduced in BMT Mice. Flt3 ligand expression was significantly greater after MI in both the W/W^v and BMT W/W^v groups. However, sham and post-MI expression of Flt3L was significantly higher in the W/W^v group compared with WT BM-rescued W/W^v mice (Fig. 5). This level of Flt3L demonstrates a previously unreported level of increase in cardiac Flt3L expression after MI, which is, in turn, much more exaggerated in c-kit-deficient mice, suggesting a potential synergetic compensatory mechanism by Flt3L in c-kit-deficient W/W^v mice, reversible with BM transplantation.

Discussion

Clinical trials using BM-derived stem/progenitor cells to improve cardiac function and remodeling after MI have attracted a lot of attention worldwide. Various groups have demonstrated the feasibility and reasonable safety of implanting these adult stem cells in injured myocardium (5–8). However, the magnitude and permanence of initial benefits observed are only being explored now in randomized trial settings (9–11). However, the mechanisms of initial improvement in cardiac function by this treatment are not well understood. Interestingly, most of the cells used in these trials or experiments have been *lin*$^-$*c-kit*$^+$ BM-derived or cardiac cells. c-kit signaling affects many target cell populations, including hematopoetic stem/progenitor cells, mast cells, and NK cells. Thus, we set out to determine the biological contribution of c-kit signaling after MI in c-kit-deficient and WT BMT-rescued mice. We have demonstrated worse cardiac function and remodeling after MI in c-kit-deficient compared with WT mice. Furthermore, we were able to rescue this adverse phenotype with matched WT BMT to levels com-

Table 1. Up-regulation of mobilization, antiapoptotic, angiogenic, and NK-related genes after MI

Category	Gene	Day 3	Day 7
Mobilization	CXCR4	3.0	2.2
	SDF1	2.0	2.1
	KITR	3.0	2.0
	KITL	2.5	2
	CXCR3	1.2	3.8
	FLT3	0	3.0
	FLT3L	2.0	0
Antiapoptotic	AKT1	2	2
	AKT2	2	2
	AKT3	2.5	1.5
	DAD1	2.0	1.7
	BAX	3.0	2.5
	TIE1	2.0	2.2
Angiogenic	TIE2	2.0	1.7
	FLT1	1.8	1.6
	VEGFC	2.1	3.0
	FLT4	1.7	1.7
	VEGFB	1.9	3.0
	FIGF	2.7	2.4
	EPHRB2	1.5	1.5
NK	CD244	1.8	1.9
	CD94	2.2	5.9
	Klra2	3.3	6.2
	Klra8	1.7	28.5
	Nkg7	1.4	11.0
	Lst1	4.2	3.9
	INF-γR2	2.4	2.3
	CXCL10	30.2	6.1
	CXCL11	8.4	5.3
	CXCL9	9.9	9.8

Fold increase at day 3 and 7 in BMT W/W^v compared with W/W^v infarcted area.

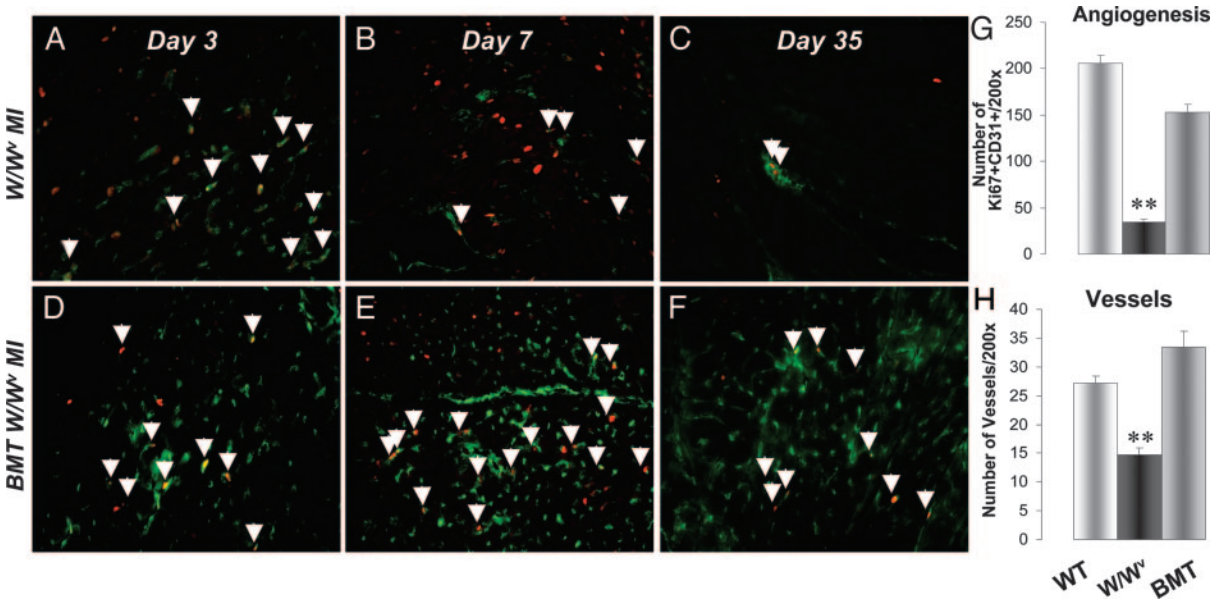

Fig. 3. Neovascularization is greatest in WT and BMT W/W^v mice. (*A–F*) CD31 (in green) and Ki67 (in red) at days 3, 7, and 35 after MI. Arrows indicate overlapping CD31 and Ki69 staining. (*G*) A significantly greater number of dividing endothelial cells at day 7 after MI is depicted. (*H*) Vessel numbers were also significantly greater in the WT and BMT W/W^v when compared with W/W^v mice. Values are mean ± SEM. **, $P < 0.001$.

parable with the WT group. We have demonstrated that BM transplantion in these mice improved cardiac function, reduced apoptosis, increased angiogenesis, and increased BM-derived cell mobilization and NK activity at early time points after MI.

Antiapoptotic paracrine activity of c-kit receptor signaling has been attributed to up-regulation of AKT cytoprotective signaling in target cells (15, 20). Activation of AKT may explain the greater survival of endothelial cells and myocytes observed in WT mice when compared with W/W^v mice. Infiltrating or resident progenitor c-kit positive cells may be contributing to this paracrine rescue signaling. Similar salutary findings have been observed by injecting AKT overexpressing mesenchymal stem cells into infarcted myocardium, leading to a reduction in infarct size (21). Our findings of reduced apoptosis in BMT W/W^v mice are consistent with the paracrine role of mobilized cells (Fig. 7).

We have also observed that WT BMT W/W^v mice demonstrated improved angiogenesis. A role for c-kit signaling in neovascularization may be expected (22) because 70% of BM-derived $CD34^+$ cells express the c-kit receptor (7, 23). Immunohistochemical colocalization of Ki67, CD31, and vessel number (Fig. 3) demonstrated increased endothelial cell proliferation and neovascularization in the BMT-rescued mice, which is also supported by gene expression analysis (Table 1). An increase in mobilization and neovascularization genes (CXCR4, MMP9, and EPHRNB2) was confirmed with real-time PCR analysis (data not shown). Although our findings demonstrated improved angiogenesis in the post-MI rescued group, there were surprisingly fewer differentiated $EGFP^+$ cells at 5 weeks, suggesting that other angiogenic mechanisms are also involved. This observation may be explained by the presence of *c-kit*$^+$ cardiac progenitor cells reported in the heart undergoing neovascularization (24, 25). These cells can also differentiate into unlabeled myocytes and, hence, were undetected by our techniques (24). These findings are supported by long-term remodeling studies performed in our laboratory. Aging W/W^v mice (9–10 months old)

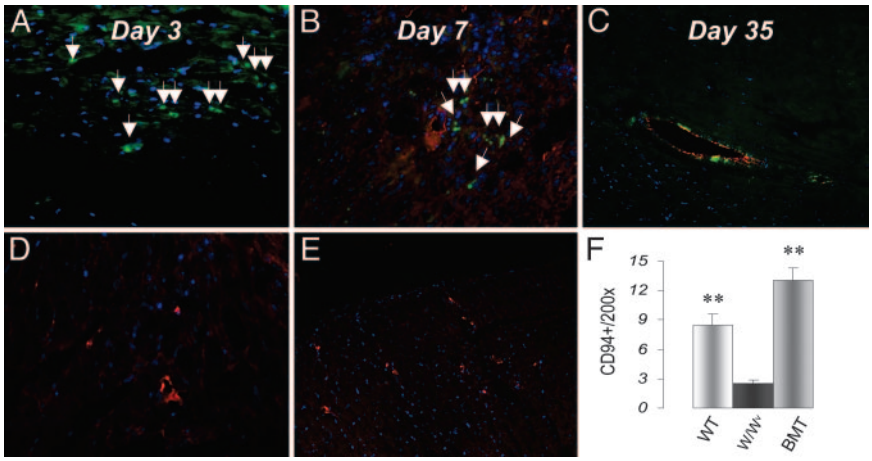

Fig. 4. Mobilization of BM-derived cells to the infarcted heart. (*A* and *B*) $EGFP^+$ cells present in BMT W/W^v mice, with maximum infiltration at days 3 and 7. (*C*) Presence of BM-derived $EGFP^+$ cells contributing to neovascularization at day 35 after MI. (*D* and *E*) CD94 inhibitory receptor staining for NK cells is present at day 3 and greatest at day 7 in BMT W/W^v. (*F*) A significantly greater number of NK cells present in WT and BMT W/W^v mice when compared with W/W^v mice at day 7 after MI. Values are mean ± SEM. **, $P < 0.001$.

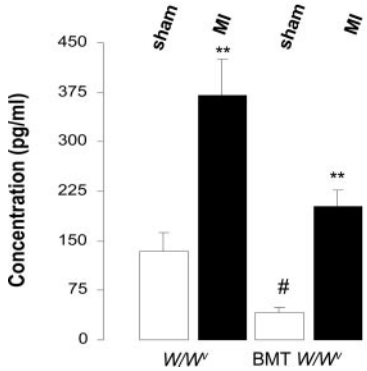

Fig. 5. Flt3L expression in whole heart W/W^v and BMT W/W^v mice ($n = 5$ each) at day 35 after MI. Significantly higher expression after MI in both groups. These levels were reduced in BMT reconstituted W/W^v sham and infarcted mice. Values are mean ± SEM. **, $P < 0.001$ and #, $P < 0.05$.

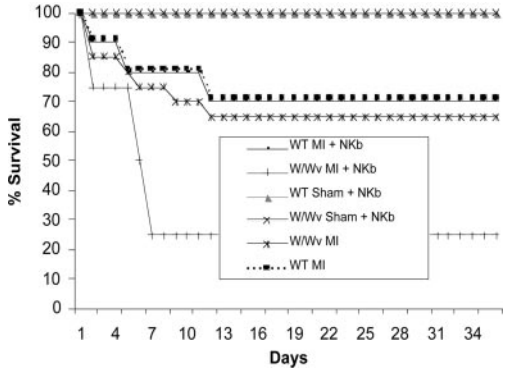

Fig. 6. W/W^v mice treated with NK blocker before MI ($n = 20$) demonstrated a 40% reduction in survival. This increase in mortality demonstrates the important remodeling role of NK cells in W/W^v mice after MI. There was no difference in survival in the WT MI mice ($n = 20$) and no changes in the sham groups ($n = 4$ each).

lead to worsening heart function in sham and infarcted mice, suggesting the presence of *c-kit*$^+$ cardiac progenitor cells and their role in cardiac remodeling (Fig. 8, which is published as supporting information on the PNAS web site). This worsening of heart function may be explained by the c-kit deficient cardiac progenitor cells in W/W^v mice preventing cell differentiation during aging or after injury.

Most importantly, our findings indicate an important role for NK cell mobilization and activity in the myocardium of BMT-rescued W/W^v mice. The importance of c-kit and its ligand, stem cell factor, in NK cell development, survival, and expansion has been demonstrated *in vivo* (18). Furthermore, the addition of stem cell factor or fetal liver kinase ligand (Flt3L) has been shown to promote NK cell differentiation from hematopoetic stem/progenitor cells *in vitro* (26). W/W^v and Flt3L null mice exhibit a reduction in number and cytotoxicity of NK cells, whereas heterozygous mutants have a reduction in the number of circulating NK cells (18, 26). We have also confirmed these observations with flow analysis of NK cells in WT and c-kit-deficient mice after MI (Fig. 9, which is published as supporting information on the PNAS web site). These results indicate the importance of c-kit and flt3 receptors in development and also mobilization of NK cells in to the circulation after MI. We believe that WT BM transplantation rescued NK cell number, mobilization, and activity in W/W^v mice and helped rescue the infarcted heart (Fig. 4 *D–F*).

The exact role and activity of NK cells in the myocardium after MI requires further investigation. One possible role of NK cells may include crosstalk with dendritic cells stimulating cytokine and chemokine release, leading to a protective paracrine effect. Borg *et al.* (16) demonstrated increased dendritic cell activity in W/W^v mice, leading to improved NK crosstalk. Furthermore, by blocking c-kit activity while administering Flt3 ligand in WT mice, they were able to phenocopy the increase in NK mobilization and activity observed in W/W^v mice (16). Flt3 receptor and ligand activity has also been further indicated in the production of NK cells (27), and increased coexpression of Flt3L in W/W^v mice has been reported (28). To investigate the role of Flt3L in our experiments, we measured the levels in W/W^v and BMT W/W^v cardiac tissue and found significantly greater Flt3L levels 35 days after MI. There was also a significant reduction in cardiac Flt3L levels in BMT W/W^v at baseline and after MI compared with W/W^v mice demonstrating a synergetic response to c-kit deficiency (Fig. 5). Our results suggest that rescued W/W^v mice have undergone repaired BM NK cell development and maturation, and with greater cardiac Flt3L expression after MI, increased mobilization into circulation and homing to the heart. In addition, in separate experiments, we have demonstrated that W/W^v mice have significantly lower numbers of peripheral NK cells and an increase in dendritic cell mobilization after MI (see Fig. 9). Using NK antibody blockers, we found a 40% reduction in survival of W/W^v mice, indicating the profound dependence on the already-low level of NK cells in these c-kit-deficient mice (Fig. 6).

We have demonstrated c-kit receptor's active role in mediating repair and remodeling after MI and in the maintenance of cardiac function. Further investigation into the paracrine role of NK cells is required and may lead to new therapeutic approaches for improving outcomes after myocardial infarction as part of an overall cardiac regeneration therapeutic strategy.

Materials and Methods

Animal Surgery and Cardiac Evaluation. W/W^v (WBB6F1-Kit^{w}Kit^{w-v}) mice are compound heterozygotes of a null *c-kit* mutation (*W*) and the *W-viable* (W^v) allele exhibiting reduced kinase activity and representing the most severe c-Kit mutants that survive gestation (14, 15). W/W^v and WT (WBB6F1) mice were purchased from The Jackson Laboratory. An LV MI was created in 10- to 12-week-old male W/W^v and WT mice by ligation of the left anterior descending coronary artery, as described in refs. 29 and 30. In experiment 1, W/W^v ($n = 12$) and WT mice ($n = 12$) underwent coronary artery ligation and were monitored for morbidity and mortality. Sham operations ($n = 8$, W/W^v; and $n = 8$, WT) were also performed as an operative control. At day 35, heart function was analyzed. In experiment 2, W/W^v ($n = 24$) and WT ($n = 24$) mice were randomized into sham-operated controls or infarction groups and randomized again for killing on days 3, 7, and 35 ($n = 6$ per time point). Hearts were harvested, rinsed with PBS (GIBCO), frozen, and stored at −80°C until analysis. In experiment 3, BM from WT mice was extracted and transduced with a lentivirus that engineers expression of EGFP (31), transplanted into irradiated W/W^v mice, and allowed to reconstitute for 3 months. Mice were then randomized into sham ($n = 22$) or infarcted groups ($n = 30$), and hearts were collected at similar time points as in experiment 1 and 2. WT-to-WT ($n = 5$) and W/W^v-to-W/W^v ($n = 5$) BMT was also performed and served as controls. In experiment 4, WT ($n = 24$) and W/W^v ($n = 26$) mice were pretreated with a rabbit anti-mouse polyclonal NK blocker (Cedarlane Laboratory, Hornby, ON, Canada) and then randomized into MI or sham groups. These mice were monitored for survival. Cardiac function of all mice surviving until day 35 was analyzed by using a Millar pressure volume conductance catheter. Morphometrics, pathology, and collagen staining were analyzed as described in refs. 29 and 30.

BM Transduction and Transplantation. To enrich for stem/progenitor cells, male WT mice were first injected i.p. for 4 days with

5-fluorouracil (150 mg/kg, Sigma). Four days later, BM cells from femoral and tibial bones were flushed and mononuclear cells (MNCs) isolated over a Nycoprep density gradient. BM MNCs were resuspended in DMEM (GIBCO) supplemented with 20% FCS (GIBCO)/6 ng/ml murine IL-3/10 ng/ml murine IL-6/100 ng/ml murine stem cell factor (all from R & D Systems). Lentivector infections were performed with concentrated virus at a multiplicity of infection of 30 in the presence of 8 μg/ml protamine sulfate (Sigma) on fibronectin-coated (5 μg/cm^2, Roche, Penzberg, Germany), nontissue culture-treated plates. After an overnight infection, adherent and nonadherent cells were harvested, washed, and resuspended in D-PBS. Approximately 1×10^6 transduced cells were transplanted intravenously into W/W^v male mice that were preconditioned with 300 cGy (110 cGy/min 37 Cs-rays by using Gamma Cell 40 from MBS Nordion) of total body irradiation. Peripheral blood from transplanted mice was collected from tail veins in K_2EDTA tubes (BD Biosciences). RBCs were lysed with RBC lysis buffer (Sigma), and flow cytometric analyses for EGFP expression and CD4, CD8, CD19, Gra-1, and CD11b (all antibodies purchased from BD Biosciences) were performed by using a FACSCalibur (BD Biosciences).

Microarray Analysis by Using Affymetrix GeneChip Hybridization. Total RNA was isolated from 18 heart samples by using TRIzol reagent (GIBCO/BRL) and following the manufacturer's protocol. The quality of RNA was assessed by an Agilent 2100 Bioanalyzer (version A.02.01S1232, Agilent Technologies, Palo Alto, CA). A total of 18 hybridizations were performed on the MG-430 or 430–2 mouse GeneChip set (Affymetrix, Santa Clara, CA) with the 18 RNAs from the infarcted region of hearts (six different groups with three replicates per group: WT days 3 and 7, W/W^v days 3 and 7, and BMT W/W^v day 3 and 7). Samples were prepared for hybridization according to standard Affymetrix instructions and performed at the Toronto Genomic Core Centre at the Hospital for Sick Children. Experimental design, gene lists, hierarchical trees, chip hybridizations, and statistical analyses were done in compliance with the Minimum Information About a Microarray Experiment guidelines (32).

Affymetrix GeneChip Data Analysis. To monitor gene expression over different time points, data obtained from the GCOS (GeneChip Operating Software) absolute analyses of all of the individual arrays were analyzed and clustered by using GENESPRING 7.0 (Agilent Technologies). After filtering, one-way ANOVA (nonequal variance) was performed and 2-fold up- or down-regulated genes in the BMT W/W^v vs. untransplanted W/W^v mice were used for hierarchical clustering. The up- or down-regulated genes in BMT W/W^v mice vs. both W/W^v and WT were used to generate the hypersensitive gene lists.

Immunohistochemistry and Collagen Content. Cryostat sections (5 μm) were cut from day 3, 7, and 35 hearts, air-dried, and fixed in cold acetone (−20°C) for 10 min. The endogenous peroxidase activity was blocked by 0.3% hydrogen peroxide (Sigma) incubated for 30 min with 10% normal rabbit/goat serum (GIBCO). Reaction with primary CD31 (BD Pharmingen), Ki67 (ID Labs, London, ON, Canada), anti-GFP (Abcam, Inc., Cambridge, MA), human von Willebrand factor VIII (Sigma), and CD94 (Biodesign International, Kennebunkport, ME) antibodies were performed overnight at 4°C and then labeled with the appropriate secondary fluorescent antibodies (Sigma). Quantification of immunoreactive cells (200 optical fields) was performed with the use of a Quantimet 600 image analysis system (Leica, Deerfield, IL) (29, 30). For collagen content, sections were stained with Sirius red 3BA in saturated picric acid solution (Sigma) and quantified with an image analysis system (Leica Q500) (29, 30).

Tissue Protein Analysis. Cardiac tissue FLT3 ligand expression was measured by using the ELISA kit (BD Biosciences). All regions of BMT W/W^v or W/W^v mice ($n = 5$ each), infarcted, peri-infarcted, and normal zones, were pooled, and heart protein concentrations were measured and compared.

Statistical Analysis. Student t tests were used to compare samples. ANOVA with Newman-Keul subgroup testing were used when multiple groups were compared. Values are expressed as mean ± SEM, with $P < 0.05$ considered significant.

We thank Dr. Thomas Podor at iCapture for microscopy guidance. This work was supported, in part, by grants from the Heart and Stroke Foundation of Ontario, the Canadian Institutes of Health Research, the Canadian Heart Failure Network Team Program, and the National Institutes of Health/National Heart, Lung, and Blood Institute (to J.A.M.). P.P.L. is the Heart and Stroke/Polo Chair Professor of Medicine and Physiology at the University of Toronto. W.L.S. is the Canada Research Chair in Stem Cell Biology and Functional Genomics. B.B.A. is a recipient of Fonds de la Recherche en Santé du Québéc Doctoral Scholarship.

1. Ryan, T. J., Antman, E. M., Brooks, N. H., Califf, R. M., Hillis, L. D., Hiratzka, L. F., Rapaport, E., Riegel, B., Russell, R. O., Smith, E. E., 3rd, *et al.* (1999) *J. Am. Coll. Cardiol.* **34,** 890–911.
2. Frangogiannis, N. G., Smith, C. W. & Entman, M. L. (2002) *Cardiovasc. Res.* **53,** 31–47.
3. Nian, M., Lee, P., Khaper, N. & Liu, P. (2004) *Circ. Res.* **94,** 1543–1553.
4. Davani, S., Deschaseaux, F., Chalmers, D., Tiberghien, P. & Kantelip, J. P. (2005) *Cardiovasc. Res.* **65,** 305–316.
5. Orlic, D., Kajstura, J., Chimenti, S., Jakoniuk, I., Anderson, S. M., Li, B., Pickel, J., McKay, R., Nadal-Ginard, B., Bodine, D. M., *et al.* (2001) *Nature* **410,** 701–705.
6. Orlic, D., Kajstura, J., Chimenti, S., Limana, F., Jakoniuk, I., Quaini, F., Nadal-Ginard, B., Bodine, D. M., Leri, A. & Anversa, P. (2001) *Proc. Natl. Acad. Sci. USA* **98,** 10344–10349.
7. Kocher, A. A., Schuster, M. D., Szabolcs, M. J., Takuma, S., Burkhoff, D., Wang, J., Homma, S., Edwards, N. M. & Itescu, S. (2001) *Nat. Med.* **7,** 430–436.
8. Jackson, K. A., Majka, S. M., Wang, H., Pocius, J., Hartley, C. J., Majesky, M. W., Entman, M. L., Michael, L. H., Hirschi, K. K. & Goodell, M. A. (2001) *J. Clin. Invest.* **107,** 1395–1402.
9. Murry, C. E., Soonpaa, M. H., Reinecke, H., Nakajima, H., Nakajima, H. O., Rubart, M., Pasumarthi, K. B., Virag, J. I., Bartelmez, S. H., Poppa, V., *et al.* (2004) *Nature* **428,** 664–668.
10. Wagers, A. J., Sherwood, R. I., Christensen, J. L. & Weissman, I. L. (2002) *Science* **297,** 2256–2259.
11. Balsam, L. B., Wagers, A. J., Christensen, J. L., Kofidis, T., Weissman, I. L. & Robbins, R. C. (2004) *Nature* **428,** 668–673.
12. Shi, D., Reinecke, H., Murry, C. E. & Torok-Storb, B. (2004) *Blood* **104,** 290–294.
13. Jiang, X., Gurel, O., Mendiaz, E. A., Stearns, G. W., Clogston, C. L., Lu, H. S., Osslund, T. D., Syed, R. S., Langley, K. E. & Hendrickson, W. A. (2000) *EMBO J.* **19,** 3192–3203.
14. Ashman, L. K. (1999) *Int. J. Biochem. Cell Biol.* **31,** 1037–1051.
15. Ronnstrand, L. (2004) *Cell. Mol. Life Sci.* **61,** 2535–2548.
16. Borg, C., Terme, M., Taieb, J., Menard, C., Flament, C., Robert, C., Maruyama, K., Wakasugi, H., Angevin, E., Thielemans, K., *et al.* (2004) *J. Clin. Invest.* **114,** 379–388.
17. Andrews, D. M., Andoniou, C. E., Scalzo, A. A., van Dommelen, S. L., Wallace, M. E., Smyth, M. J. & Degli-Esposti, M. A. (2005) *Mol. Immunol.* **42,** 547–555.
18. Colucci, F., Caligiuri, M. A. & Di Santo, J. P. (2003) *Nat. Rev. Immunol.* **3,** 413–425.
19. Raulet, D. H. (2004) *Nat. Immunol.* **5,** 996–1002.
20. Smith, M. A., Court, E. L. & Smith, J. G. (2001) *Blood Rev.* **15,** 191–197.
21. Mangi, A. A., Noiseux, N., Kong, D., He, H., Rezvani, M., Ingwall, J. S. & Dzau, V. J. (2003) *Nat. Med.* **9,** 1195–1201.
22. De Waele, M., Renmans, W., Asosingh, K., Vander Gucht, K. & Van Riet, I. (2004) *Eur. J. Haematol.* **72,** 193–202.
23. Lanza, R., Moore, M. A., Wakayama, T., Perry, A. C., Shieh, J. H., Hendrikx, J., Leri, A., Chimenti, S., Monsen, A., Nurzynska, D., *et al.* (2004) *Circ. Res.* **94,** 820–827.
24. Beltrami, A. P., Barlucchi, L., Torella, D., Baker, M., Limana, F., Chimenti, S., Kasahara, H., Rota, M., Musso, E., Urbanek, K., *et al.* (2003) *Cell* **114,** 763–776.
25. Schuster, M. D., Kocher, A. A., Seki, T., Martens, T. P., Xiang, G., Homma, S. & Itescu, S. (2004) *Am J. Physiol.* **287,** H525–H532.
26. Colucci, F. & Di Santo, J. P. (2000) *Blood* **95,** 984–991.
27. Drexler, H. G. & Quentmeier, H. (2004) *Growth Factors* **22,** 71–73.
28. Omori, M., Omori, N., Evarts, R. P., Teramoto, T. & Thorgeirsson, S. S. (1997) *Am. J. Pathol.* **150,** 1179–1187.
29. Sun, M., Dawood, F., Wen, W. H., Chen, M., Dixon, I., Kirshenbaum, L. A. & Liu, P. P. (2004) *Circulation* **110,** 3221–3228.
30. Sun, M., Opavsky, M. A., Stewart, D. J., Rabinovitch, M., Dawood, F., Wen, W. H. & Liu, P. P. (2003) *Circulation* **107,** 1046–1052.
31. Yoshimitsu, M., Sato, T., Tao, K., Walia, J. S., Rasaiah, V. I., Sleep, G. T., Murray, G. J., Poeppl, A. G., Underwood, J., West, L., Brady, R. O. & Medin, J. A. (2004) *Proc. Natl. Acad. Sci. USA* **101,** 16909–16914.
32. Brazma, A., Hingamp, P., Quackenbush, J., Sherlock, G., Spellman, P., Stoeckert, C., Aach, J., Ansorge, W., Ball, C. A., Causton, H. C., *et al.* (2001) *Nat. Genet* **29,** 365–371.